

RESEARCH ARTICLE



Small G protein signalling modulator 2 (SGSM2) is involved in oestrogen receptor-positive breast cancer metastasis through enhancement of migratory cell adhesion via interaction with E-cadherin

Juo-Han Lin^a, Wen-Jui Lee^b, Han-Chung Wu^c, Chih-Hsiung Wu^{d,e}, Li-Ching Chen^{f,g,h}, Chi-Cheng Huang^{d,i,j}, Hang-Lung Chang^e, Tzu-Chun Cheng^k, Hui-Wen Chang^l, Chi-Tang Ho^m, Shih-Hsin Tu^{d,f,g}, and Yuan-Soon Ho^{h,k,l,n}

^aPh.D. Program for Cancer Molecular Biology and Drug Discovery, College of Medical Science and Technology, Taipei Medical University and Academia Sinica, Taipei, Taiwan; ^bPh.D. Program for Neural Regenerative Medicine, College of Medical Science and Technology, Taipei Medical University and National Health Research Institutes, Taipei, Taiwan; ^cInstitute of Cellular and Organismic Biology, Academia Sinica, Taipei, Taiwan; ^dDepartment of Surgery, School of Medicine, College of Medicine, Taipei Medical University, Taipei, Taiwan; ^eDepartment of General Surgery, En Chu Kong Hospital, New Taipei City, Taiwan; ^fBreast Medical Center, Taipei Medical University Hospital, Taipei, Taiwan; ^gTaipei Cancer Center, Taipei Medical University, Taipei, Taiwan; ^hTMU Research Center of Cancer Translational Medicine, Taipei Medical University, Taipei, Taiwan; ⁱSchool of Medicine, College of Medicine, Fu-Jen Catholic University, New Taipei City, Taiwan; ^jDepartment of Surgery, Fu-Jen Catholic University Hospital, New Taipei City, Taiwan; ^kSchool of Medical Laboratory Science and Biotechnology, College of Medical Science and Technology, Taipei Medical University, Taipei, Taiwan; ^lDepartment of Laboratory Medicine, Taipei Medical University Hospital, Taipei, Taiwan; ^mDepartment of Food Science, Rutgers University, New Brunswick, NJ, USA; ⁿGraduate Institute of Medical Sciences, College of Medicine, Taipei Medical University, Taipei, Taiwan

ABSTRACT

The function of small G protein signalling modulators (SGSM1/2/3) in cancer remains unknown. Our findings demonstrated that SGSM2 is a plasma membrane protein that strongly interacted with E-cadherin/ β -catenin. SGSM2 downregulation enhanced the phosphorylation of focal adhesion kinase (FAK; Y576/577), decreased the expression of epithelial markers such as E-cadherin, β -catenin, and Paxillin, and increased the expression of Snail and Twist-1, which reduced cell adhesion and promoted cancer cell migration. Oestrogen and fibronectin treatment was found to promote the colocalization of SGSM2 at the leading edge with phospho-FAK (Y397). The BioGRID database showed that SGSM2 potentially interacts with cytoskeleton remodelling and cell-cell junction proteins. These evidences suggest that SGSM2 plays a role in modulating cell adhesion and cytoskeleton dynamics during cancer migration.

ARTICLE HISTORY

Received 15 July 2018
Revised 13 December 2018
Accepted 2 January 2019

KEYWORDS

SGSM; breast cancer; cell adhesion; E-cadherin; oestrogen receptor; EMT

Introduction

A distinct metastatic pattern is one characteristic of breast cancer (BC); metastasis often occurs in the lymph nodes, bone, lung, and liver, leading to a high death rate. Tumour cell metastasis and invasion are complicated processes involving multiple steps; recently, the most commonly described step of metastasis initiation is the epithelial-mesenchymal transition (EMT) [1]. EMT is a complex process that occurs in wound healing, organ fibrosis, or the initiation of cancer metastasis. During this process, cells first lose cell-cell adhesion through disruption of E-cadherin-mediated junctions, and then increased cell motility via interplay between the actin cytoskeleton and cell adhesion sites leads to the generation of membrane protrusions and traction forces [2–5].

Migration inducers include fibroblast growth factor (FGF), transforming growth factor β (TGF- β), epidermal growth factor (EGF), insulin-like growth factor-1 (IGF1), tumour necrosis factor- α (TNF α), and Wnt/ β -catenin, and the regulation of EMT transcription factors, such as Snail and Twist [6–9], which drive cell movement by direct repression of E-cadherin cell adhesion molecule transcription. In addition, the upregulation of proteases, such as matrix metalloproteinases (MMPs), can also disrupt E-cadherin/catenin-mediated cell-cell adhesion [10,11], and hepatocyte growth factor/scatter factor (HGF/SF), a multifunctional cytokine that is secreted by mesenchymal cells in the tumour microenvironment, can downregulate E-cadherin and induce pro-migratory small G proteins (small GTPases), such as Ras, Rho/Rac, and Ras-associated protein (Rap)

CONTACT Yuan-Soon Ho  hoyuansn@tmu.edu.tw  School of Medical Laboratory Science and Biotechnology, College of Medical Science and Technology, Taipei Medical University, No. 250 Wu-Hsing Street, Taipei 110, Taiwan; Shih-Hsin Tu  drtu@h.tmu.edu.tw  Breast Medical Center, Taipei Medical University Hospital, No. 252, Wu-Hsing Street, Taipei 110, Taiwan
 Supplemental data for this article can be accessed [here](#).

[5,12,13]. The activation of small GTPases increases cell motility and migration not only through the promotion of membrane trafficking but also through the control of cytoskeletal reorganization and cell adhesion [14,15].

A novel group of small G protein signalling modulators (SGSM1/2/3) were first reported in 2007 [16]. TBC and RUN motifs are two major conserved domains of the SGSM family and appear to be related to the modulation of the small GTPases RAP and RAB, which mediate signal transduction and vesicular transportation pathways [16–18]; additionally, a RAP-interacting domain (RAPID) motif among all the SGSMS was identified as the true interaction site between SGSM and the RAP family (RAP1A/1B/2A/2B) [16]. Many studies have indicated that RAP proteins play an important role in the formation of cadherin-based cell-cell junctions, especially RAP1, which regulates adhesion and migration in many cancers via shuttling between its inactive GDP- and active GTP-bound form [19–21]. Currently, the role of SGSM proteins in cancer is still unknown, but SGSM proteins have been identified as GTPase-activating proteins (GAPs), which can modulate G protein signalling by interacting with RAP and RAB family proteins [22,23]. Therefore, this study aims to determine whether SGSM proteins participate in BC carcinogenesis and to identify the underlying mechanisms.

According to our first screening, *SGSM1* mRNA was not expressed in BC or breast epithelial cells, and compared with *SGSM2* expression, *SGSM3* expression was not different between normal breast tissue and tumour tissues based on RT-PCR. We consequentially narrowed our focus to *SGSM2* and investigated its function in BC. Real-time PCR data revealed that *SGSM2* mRNA was more highly expressed in ER-positive malignant tissues than in ER-negative tissues from 200 BC patients, and its protein expression was also associated with ER-positive BC cells. Interestingly, we found that trypsin could cleave *SGSM2* protein on the plasma membrane, which was confirmed by a cytosol and membrane extraction assay. This novel finding indicated that *SGSM2* is a plasma membrane protein. Consistently, knock-down of *SGSM2* by small interfering RNA (siRNA) induced the phosphorylation of focal adhesion kinase (FAK; Y576/577), a decrease in the expression of the epithelial markers E-cadherin, β -catenin, and Paxillin, and an increase in the expression of upstream epithelial markers Snail and Twist-1, which led to a reduction in cell adhesion and the promotion of cancer cell migration. In addition, *SGSM2* was found

to exhibit a strong interaction with E-cadherin/ β -catenin cell junction complexes, even in the presence of EGTA (4 mM), which inhibits the formation of this complex, and in the presence of EGF (100 nM), which induces E-cadherin endocytosis. *SGSM2* was also found to participate in oestrogen- and fibronectin-induced cell migration, and colocalization with phospho-FAK (Tyr397) was clearly observed at the leading edge at the beginning of cell migration. The prediction from the BioGRID database showed that *SGSM2* potentially interacts with cytoskeleton remodelling and cell-cell junction proteins, including formin-binding protein 1-like (FNBP1L), Wiskott-Aldrich syndrome-like (WASL), cell division cycle 42 (CDC42), and cadherin 1 (CDH1). These novel findings demonstrate that *SGSM2* may be involved in the modulation of cell adhesion and cytoskeleton dynamics through an E-cadherin-mediated EMT process during the initial stage of cancer migration.

Results

SGSM2 mRNA expression was associated with luminal a breast cancer rather than HER2-enriched or basal-like breast cancer

To determine whether *SGSM2* expression correlated with BC, we randomly detected the *SGSM2* mRNA level in 53 BC sample tissues via RT-PCR, as shown in Figure 1(a). Among 53 BC patients, 74% had *SGSM2* mRNA expression in tumours that was higher than that in normal tissue ($T > N$, $n = 39$), but in 26% of patients, *SGSM2* mRNA expression in tumour tissue was less than that in normal tissue ($N > T$, $n = 14$). The mean of the fold difference in the $T > N$ group (8.62-fold) was higher than that in the $N > T$ group (4.57-fold) (Figure 1(a), Chi-square goodness-of-fit test, $***P < 0.001$). We further evaluated *SGSM2* mRNA in 200 paired normal and malignant breast tissues using real-time PCR (Figure 1(b,c)). *SGSM2* expression was observed more often in early cycles in tumour tissues (red lines) than in normal tissues (green lines) (Figure 1(b)), and the average *SGSM2* copy number in paired tumour tissues was 2-fold higher than that in paired normal tissues (Figure 1(c), bar 2 vs. bar 1 = 213.2 vs. 108.3; $**P = 0.002$). Statistical analysis of the correlation between *SGSM2* and the clinical status of the tumour tissues is shown in Table 1. The copy number was transformed into \log_2 (copy number +1) values. *SGSM2* had significantly higher expression in ER+, PR+, HER2 – breast tumours than in ER–, PR–, HER2+ tumours (Tukey HSD test, $*P = 0.046$; Table 1), and an elevated *SGSM2* mRNA level was found in

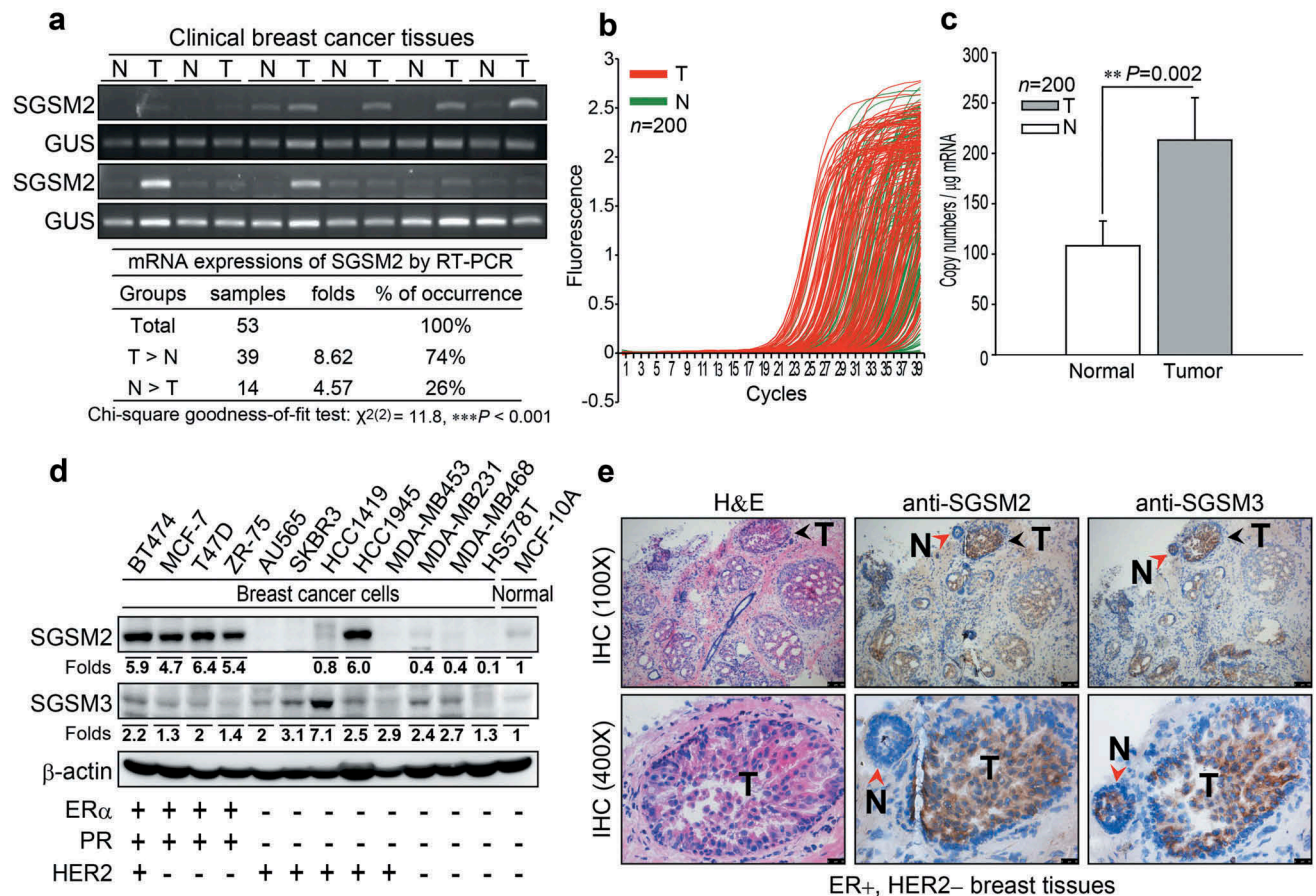


Figure 1. *SGSM2* expression was detected in human breast tissues and human breast cancer cell lines. (a) *SGSM2* mRNA expressions in normal and malignant tissues was determined in 53 BC patients via RT-PCR, and the gel band intensities were quantified with PhotoCaptMw software (version 11.0.). We used normalized *SGSM2* expression to classify patients into three groups: T > N, N = T, and N > T (N = normal tissue, and T = tumour tissue); and further, (b) quantitative real-time PCR was used to evaluate *SGSM2* mRNA expression profiles in paired human breast tumour (red lines) and normal (green lines) tissues ($n = 200$). (c) The means of *SGSM2* mRNA copy number (per μg of mRNA) were calculated from real-time PCR data. The data were analysed with a paired sample t -test with two-sided P -values. (d) *In vitro* *SGSM2* and *SGSM3* protein expression was detected in twelve breast cancer cell lines and one breast epithelial cell line; the mean density of *SGSM2* and *SGSM3* protein level in each cell line was normalized to β -actin, and the values were compared to the MCF-10A cell line. The hormone receptor status is displayed at the bottom. (e) The distribution of *SGSM2* and *SGSM3* proteins were determined in ER+/HER2- breast cancer tissue sections; Haematoxylin (violet, for nuclei) and eosin (pink) (H&E) staining is shown in the left panels; anti-*SGSM2* and anti-*SGSM3* antibody bound to antigen is shown in the middle and right panels (N = normal region, T = tumour region). Top panels: 100x, scale bar: 100 μm ; bottom panels: 400x, scale bar: 25 μm .

well-differentiated tumours (Grade 1) but not in poorly differentiated tumours (Grade 3); however, the results were non-significant (Table 1). To confirm these observations, the *SGSM2* mRNA level obtained using RNAseq data of the TCGA Breast Cancer (BRCA) cohort via UCSC Xena browser (<http://xena.ucsc.edu>) was calculated (Supplementary Table 1). The *SGSM2* mRNA level correlated with ER+, PR+, and HER2- BC ($***P < 0.001$; Supplementary Table 1), and increased *SGSM2* mRNA expression was predominately detected in tissue samples from patients with luminal A type BC compared with HER2-enriched and basal-like BC patients (Scheffe test, $***P < 0.001$). Box plots showing

SGSM2 mRNA levels associated with ER status and PAM50 subtype are provided in Figure S1(a-d).

***SGSM2* protein expression in ER-positive breast cancer**

Next, we examined *SGSM2* and *SGSM3* protein expression in 12 BC cell lines (BT474, MCF-7, T-47D, ZR-75, AU565, SKBR3, HCC1419, HCC1945, MDA-MB453, MDA-MB231, MDA-MB468, and HS578T) and one breast epithelial cell line (MCF-10A) (Figure 1(d)). Compared with *SGSM3*, *SGSM2* was not generally expressed in all cells; it appeared to be primarily expressed

Table 1. Clinical *SGSM2* mRNA expression status was detected with real-time PCR in tumour samples.

| <i>SGSM2</i> | | | | <i>SGSM2</i> | | | | |
|-------------------------|-------------------------------|-----------------------|----------------|-----------------------|-------------------------------|-----------------------|-------------|-------------|
| Factors | Copy number (Mean ± S.E.M) | Statistics P-value | Case Number | Factors | Copy number (Mean ± S.E.M) | Statistics P-value | Case Number | |
| ER status | Student's t-test | P = 0.320 | Total = 152 | Radiotherapy | Student's t-test | P = 0.070 | Total = 96 | |
| Negative | 4.74 ± 0.41 | | 45 | non-treatment | 4.95 ± 0.34 | | 75 | |
| positive | 5.27 ± 0.29 | | 107 | post-treatment | 3.65 ± 0.56 | | 21 | |
| PR status | Welch's t-test | P = 0.129 | Total = 151 | Chemotherapy | Welch's t-test | P = 0.979 | Total = 108 | |
| Negative | 4.74 ± 0.29 | | 68 | non-treatment | 5.11 ± 0.51 | | 35 | |
| positive | 5.45 ± 0.36 | | 83 | post-treatment | 5.09 ± 0.38 | | 73 | |
| HER2 status | Student's t-test | P = 0.121 | Total = 134 | Hormonotherapy | Student's t-test | P = 0.674 | Total = 111 | |
| Negative | 5.64 ± 0.32 | | 94 | non-treatment | 4.93 ± 0.48 | | 37 | |
| positive | 4.76 ± 0.44 | | 40 | post-treatment | 5.20 ± 0.37 | | 74 | |
| Menopause | Student's t-test | P = 0.968 | Total = 61 | Target therapy | Student's t-test | P = 0.629 | Total = 91 | |
| No | 6.48 ± 0.81 | | 16 | non-treatment | 5.46 ± 0.37 | | 77 | |
| Yes | 6.52 ± 0.48 | | 45 | post-treatment | 5.00 ± 0.87 | | 14 | |
| Receptor subtype | ANOVA | P = 0.070 | Total = 134 | Grade | ANOVA | No Homogeneity | Total = 144 | |
| ER+PR+HER2- | 5.78 ± 0.38 | Tukey HSD | 72 | Grade 1 | 4.97 ± 0.43 | | 37 | |
| ER+PR+HER2+ | 5.65 ± 0.66 | | 21 | Grade 2 | 5.50 ± 0.38 | | 76 | |
| ER-PR-HER2+ | 3.77 ± 0.20 | | * 0.046 | 19 | Grade 3 | 4.32 ± 0.42 | | 31 |
| Triple negative | 5.17 ± 0.53 | | | 22 | N status | ANOVA | P = 0.822 | Total = 158 |
| Stage | ANOVA | P = 0.623 | Total = 158 | N0 | 5.21 ± 0.36 | | 72 | |
| stage 0 | 3.80 ± 0.73 | | 3 | N1 | 4.91 ± 0.35 | | 54 | |
| stage I | 5.58 ± 0.51 | | 37 | N2 | 5.86 ± 1.18 | | 9 | |
| stage II | 4.91 ± 0.30 | | 82 | N3 | 5.22 ± 0.76 | | 19 | |
| stage III | 5.51 ± 0.63 | | 27 | M status | Student's t-test | P = 0.896 | Total = 157 | |
| stage IV | 4.46 ± 1.81 | | 5 | M0 | 5.01 ± 0.24 | | 144 | |
| T status | ANOVA | P = 0.690 | Total = 155 | M1 | 4.88 ± 0.84 | | 9 | |
| T1 | 5.25 ± 0.43 | | 52 | | | | | |
| T2 | 5.10 ± 0.31 | | 89 | | | | | |
| T3 | 4.63 ± 0.83 | | 9 | | | | | |
| T4 | 2.00 ± 0.00 | | 1 | | | | | |

The copy number is displayed as the log₂ (copy number +1) value. Independent t-tests (Welch's t-test for heterogeneous variances) were used to compare differences between two groups, and one-way ANOVA (Tukey HSD test) was used to compare differences among three or more groups. Quantitative data are presented as the mean ± S.E.M; the mean is the average log₂ (*SGSM2* copy number +1) value. All P-values are two-tailed, and * indicates statistical significance with P ≤ 0.05.

in ER-positive BC cells (BT474, MCF-7, T-47D, and ZR-75) and HCC1945 (Figure 1(d)). Positive *SGSM2* staining in tumours compared with normal cells was confirmed by IHC in ER+/HER2 – BC tissue sections (Figure 1(e), middle panels). However, *SGSM3* was homogeneously expressed in both tumour and normal tissues (Figure 1(e), right panels). These preliminary data revealed that *SGSM2* expression was stronger in BC with the ER-positive phenotype.

Trypsin-EDTA disrupted *SGSM2* protein expression on the plasma membrane

The typical trypsin-EDTA concentration used to detach cells adhered to culture dishes is ~21 μM. Because *SGSM2* protein was incidentally found to be digested by trypsin-EDTA, to verify this observation, adherent T47D cells were treated with different trypsin concentrations (0, 2.63, 5.25, 10.5, and 21 μM) for 3 minutes (Figure S2(a)). These concentrations were sufficiently high to destroy *SGSM2* protein; therefore, we diluted the trypsin-EDTA concentration to 0, 0.21, 2.1, 21, 210, or 2100 nM; the results shown in Figure 2(a). Interestingly, *SGSM2* protein disappeared when the cells were treated with trypsin-EDTA at concentrations higher than 21 nM; however, *SGSM3* protein expression

did not exhibit concentration-dependent differences (Figure 2(a)). Similar results were obtained using another protease (chymotrypsin). Treatment with chymotrypsin at several concentrations (1, 5, 10, 50, and 100 μg/ml) also completely degraded *SGSM2* protein within 5 minutes (Figure S2(c,d)). Next, we treated a panel of adherent breast cancer cell lines and a human melanoma cell line (MDA-MB-435 s) with or without 21 μM trypsin-EDTA and analysed *SGSM2* protein by western blot (Figure 2(b)). *SGSM2* protein nearly vanished after trypsin treatment, and E-cadherin, a cell membrane marker, was also affected by trypsin; only *SGSM3* remained present (Figure 2(b)). Next, we demonstrated that *SGSM2* protein was significantly regenerated 6 hours after cell seeding when using 1X (21 μM) trypsin-EDTA, and E-cadherin was renewed at an earlier time (Figure 2(c)). Notably, the formation of 55-kDa *SGSM2* protein fragments exhibited a time-dependent decrease after trypsin-EDTA treatment of T47D cells (Figure S2(e)). Trypsin can breakdown the proteins responsible for surface adherence during cell passaging; thus, cytosol and membrane extraction experiments were performed to clarify whether *SGSM2* protein was located at the plasma membrane. Surprisingly, we found that *SGSM2* was present in the plasma membrane along with EGFR, while both were

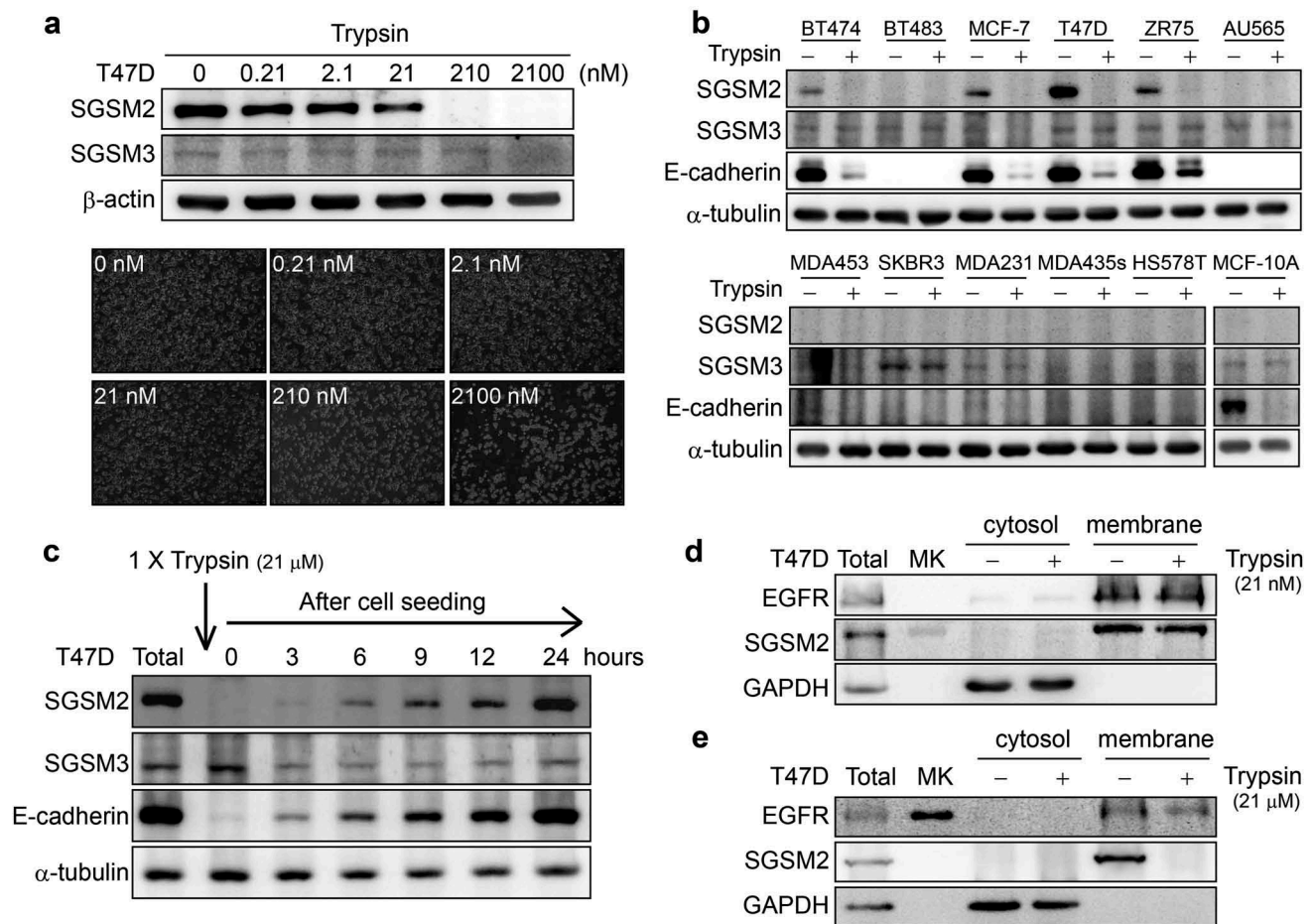


Figure 2. Trypsin-EDTA-digested SGSM2 protein on the cell membrane in the T47D breast cancer cell line. (a) T47D cells were treated with different concentrations (0, 0.21, 2.1, 21, 210, or 2100 nM) of trypsin-EDTA for 3 minutes; bottom graphs show different cell morphologies after trypsin-EDTA treatment (5x, scale bar: 250 μ m). (b) SGSM2, E-cadherin, and SGSM3 protein expression changes were observed in 11 adherent breast cell lines and a human melanoma cell line (MDA-MB-435s) after treatment with or without trypsin-EDTA (21 μ M). (c) T47D cells were treated with trypsin-EDTA (1X; 21 μ M) for subculture, and then, SGSM2, E-cadherin, and SGSM3 protein levels were observed at different time points (0, 3, 6, 9, 12, and 24 hours) after cell seeding. (d) Cytosol and membrane extracts were examined to confirm SGSM2 protein localization after 21 nM trypsin-EDTA treatment, and (e) higher (21 μ M) trypsin-EDTA concentrations were further examined. 'Total', representing total protein, which was the positive control, was extracted after cell seeding for 48 hours. GAPDH and EGFR were used as the positive cytosol and membrane controls, respectively. α -Tubulin served as the internal control for western blotting.

absent from the cytosolic extract (Figure 2(d,e)). Furthermore, compared with a low-dose (21 nM) trypsin treatment, a high dose (21 μ M) of trypsin disturbed this phenomenon (Figure 2(d vs. e)). The above evidence reliably confirms that SGSM2 is located on the plasma membrane, and our study is the first to report such an observation.

Treatment of T47D cells with trypsin affected cell adhesion ability

Because SGSM2 is a plasma membrane protein, its function needs to be clarified. We first selected the optimal concentration of extracellular matrix (ECM) proteins, such as fibronectin, type I collagen, and type IV collagen, for cell adhesion assays. Then, an enzyme-free cell

dissociation buffer rather than trypsin was used to detach T47D cells to ensure that the SGSM2 protein structure was not affected. Figure 3(a) shows that the most significant difference between treatment with dissociation buffer and treatment with trypsin occurred in the fibronectin-coated group, especially at concentrations of 0.1 and 1 μ g/ml fibronectin (**P = 0.002, and **P < 0.01); therefore, 1 μ g/ml fibronectin was chosen to coat the dish for the following experiments. Nicotine and NNK have been documented as a co-carcinogen and carcinogen, respectively, that promote cancer formation and increase the risk of cancer invasion [24,25]. Enhancement of focal adhesion ability is one characteristic that facilitates cancer cell migration. Next, we wished to clarify whether trypsin treatment would affect nicotine- or NNK- induced cell adhesion. We harvested cells with cell dissociation buffer

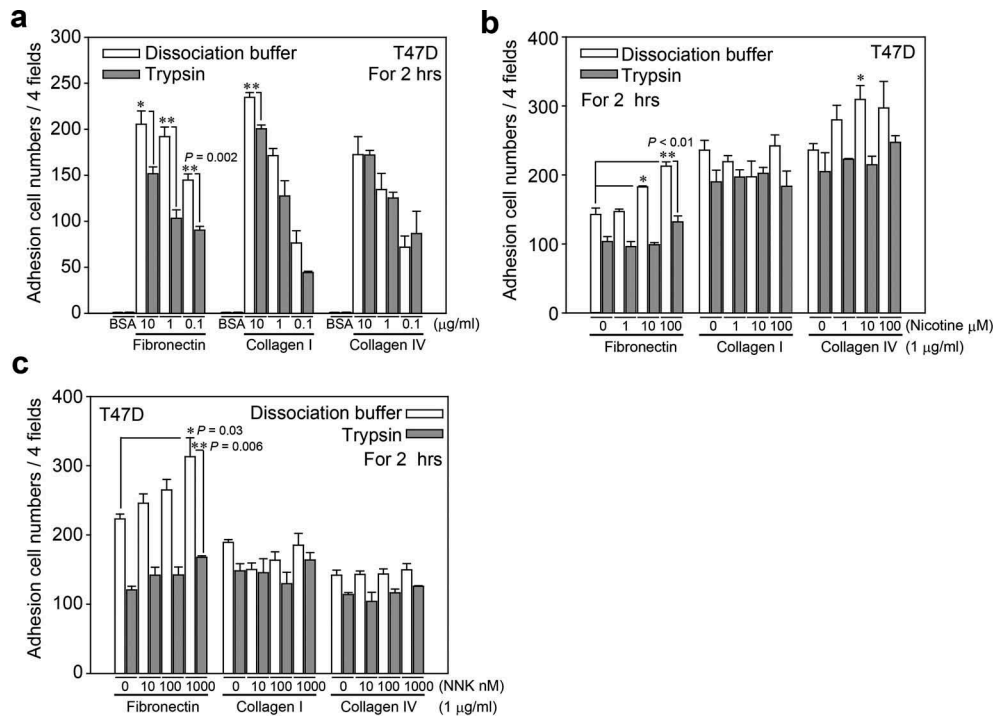


Figure 3. The cell adhesion ability of T47D cells on different ECM proteins was determined. (a) Using different concentrations (0.1, 1, and 10 µg/ml) of three types (fibronectin, type I, and type IV collagens) of ECM proteins, cell adhesion ability between cell dissociation buffer- and trypsin-EDTA (1X; 21 µM)-detached T47D cells was assessed. The BSA group was the negative control. Finally, we chose a 1 µg/ml dose of ECM proteins for the following experiments. (b) (c) Different concentrations (0, 1, 10, and 100 µM) of nicotine and NNK (0, 10, 100, and 1000 nM) were used to determine the influence the adhesion ability of dissociation buffer- and trypsin-detached T47D cells cultured on three types of ECM proteins (1 µg/ml). P-values were determined with Student's t-test; * $P < 0.05$ and ** $P < 0.01$. All experiments were repeated more than 3 times ($n > 3$).

and found that the average number of adherent cells was dose-dependently (0, 1, 10, 100 µM) increased in the fibronectin (1 µg/ml) group after treatment with nicotine (Figure 3(b), bar 1 vs. 7 and bar 7 vs. 8; ** $P < 0.01$, bar 1 vs. 5; * $P = 0.013$). However, this result was not observed after treating the cells with trypsin. The same phenomenon was observed after treatment with different doses (0, 10, 100, 1000 nM) of NNK (Figure 3(c), bar 1 vs. 7; * $P = 0.03$, bar 7 vs. 8; ** $P = 0.006$), and the result was more significant for exposure to NNK than for exposure to nicotine.

Calebin A decreased SGSM2 protein levels and inhibited cancer cell adhesion ability

According to the above-described data, trypsinization of adherent cells may disrupt SGSM2 protein on the plasma membrane (Figure 2) and decrease cell adhesion ability (Figure 3). However, because trypsin exposure affects not only SGSM2 protein but also other cell membrane proteins, we screened several natural compounds for the specific inhibition of SGSM2 protein. SGSM2 mRNA levels were decreased by treatment with 10 µM calebin A for 24 hours, and the results are

shown in Figure 4(a). Figure 4(b) shows that calebin A and 3' PS (10 µM) more strongly repressed SGSM2 protein. The cell adhesion ability in the calebin A (10 µM) combined with NNK (100 nM) group was significantly suppressed compared with the DMSO group (Figure 4(c), bar 2 vs. 4; ** $P < 0.01$). Additionally, 3' PS (10 µM) treatment also inhibited the NNK-induced increase in cell adhesion ability (Figure 4(c), bar 2 vs. 6; * $P = 0.015$). T47D cells were further treated with different concentrations (0, 0.1, 1, or 10 µM) of calebin A for 24 hours. Calebin A at 1 µM was able to inhibit SGSM2 protein levels; however, treatment with 10 µM calebin A produced more significant results (Figure 4(d)). Furthermore, cotreatment with NNK and 1 µM or 10 µM calebin A significantly suppressed NNK-induced cell adhesion (Figure 4(e), bar 2 vs. 6; ** $P = 0.003$, bar 2 vs. 8; ** $P = 0.007$).

SGSM2 silencing decreased breast cancer cell adhesion and promoted cell migration

Although calebin A decreased SGSM2 protein levels and inhibited NNK-induced cell adhesion (Figure 4), these findings do not demonstrate that SGSM2 is

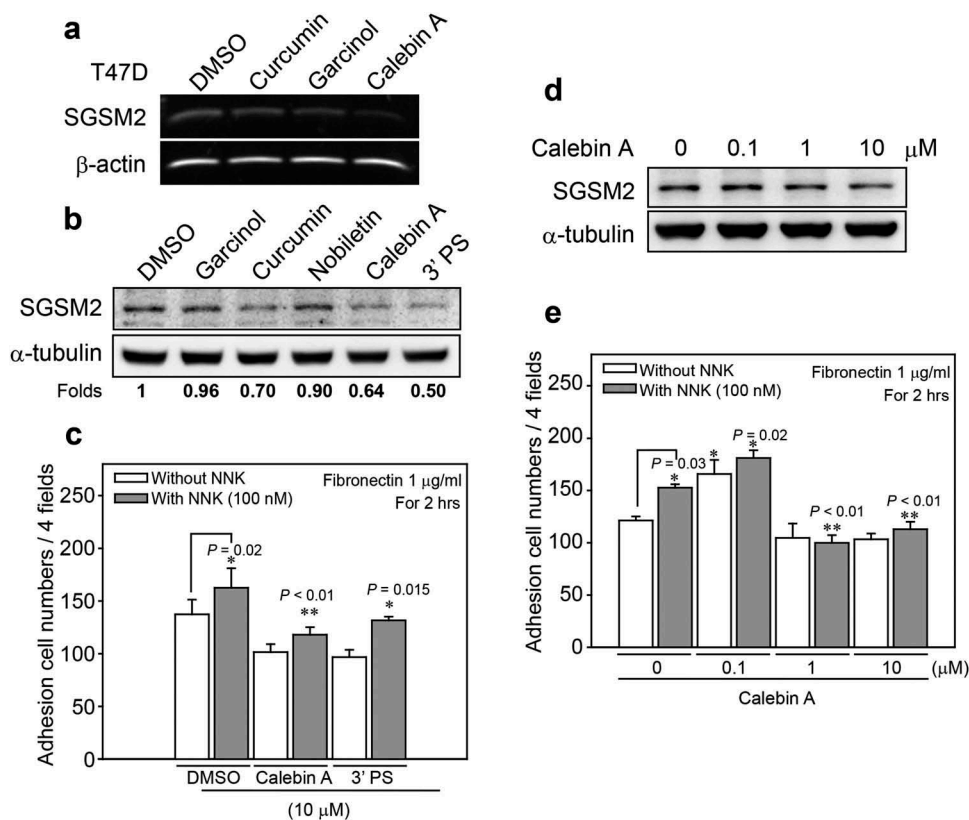


Figure 4. Natural compounds inhibited SGSM2 protein expression and decreased NNK-induced cell-matrix adhesion. (a) Determination of SGSM2 mRNA levels after treatment with 10 μ M of several natural compounds (curcumin, garcinol, and calebin A) for 24 hours (b) Determination of the SGSM2 protein levels after treatment with 10 μ M of various natural compounds (garcinol, curcumin, nobiletin, calebin A, and 3' PS) for 24 hours; DMSO was the solvent control. The mean density of SGSM2 protein level in each cell line was normalized to α -tubulin, and the values were compared with DMSO. (c) Differences in T47D cell adhesion abilities were investigated by treatment with two (calebin A and 3' PS; 10 μ M) natural compounds combined with or without NNK (100 nM). (d) SGSM2 proteins were dose-dependently decreased by treatment with calebin A (0, 0.1, 1, and 10 μ M) for 24 hours. (e) NNK (100 nM)-induced cell adhesion abilities were significantly inhibited by cotreatment with 1 and 10 μ M calebin A. For adhesion experiments, 1 μ g/ml fibronectin was coated onto the dish. α -Tubulin was the internal control. P-values were determined with Student's *t*-test; **P* < 0.05, and ***P* < 0.01. All experiments were repeated more than 3 times (*n* > 3).

involved in regulating cancer cell adhesion. We next established stable SGSM2 expression, knockdown and scramble T47D cell lines. Two pSUPER siSGSM2 (si1 and si2) and one pSUPER scramble colonies were selected for the following experiments (Figure 5(a), upper panel). The cell shape upon SGSM2 silencing was observed by bright field microscopy, as shown in Figure S3. Compared with wild-type and scramble T47D cells, which exhibited a round and aggregate shape (Figure S3(a,b)), cells of the SGSM2 si1 displayed a flattened and more spindle morphology (Figure S3(c)). In addition, the cell adhesion ability of the si2 SGSM2 cells was not significantly different from that of wild-type or scramble cells. However, si1 SGSM2, with almost complete inhibition of SGSM2 expression, exhibited significantly decreased cell adhesion in the fibronectin group (Figure 5(a), sc vs. si1;

***P* < 0.01, *n* > 3). A wound-healing assay showed that SGSM2 knockdown may increase BC cell migration (Figure 5(b)). The left panels show that si1 SGSM2 cells migrated quickly at 24 hours, and at 48 hours, the cells appeared to close the wound gap. The cell numbers are shown in the right panels (Figure 5(b), wild-type (wt) vs. si1; ***P* = 0.006, *n* > 3). EMT is a biological process in which a non-motile epithelial cell converts to a mesenchymal phenotype with invasive capacity [26] through molecular changes that decrease cell-cell recognition and adhesion and increase the potential for cell motility [1]; therefore, changes in EMT-associated markers can be used to identify this phenomenon. Certain epithelial markers, such as E-cadherin, β -catenin, and Paxillin, were decreased in si1 SGSM2 T47D cells. In contrast, the phosphorylation of FAK (Y576/577) was significantly

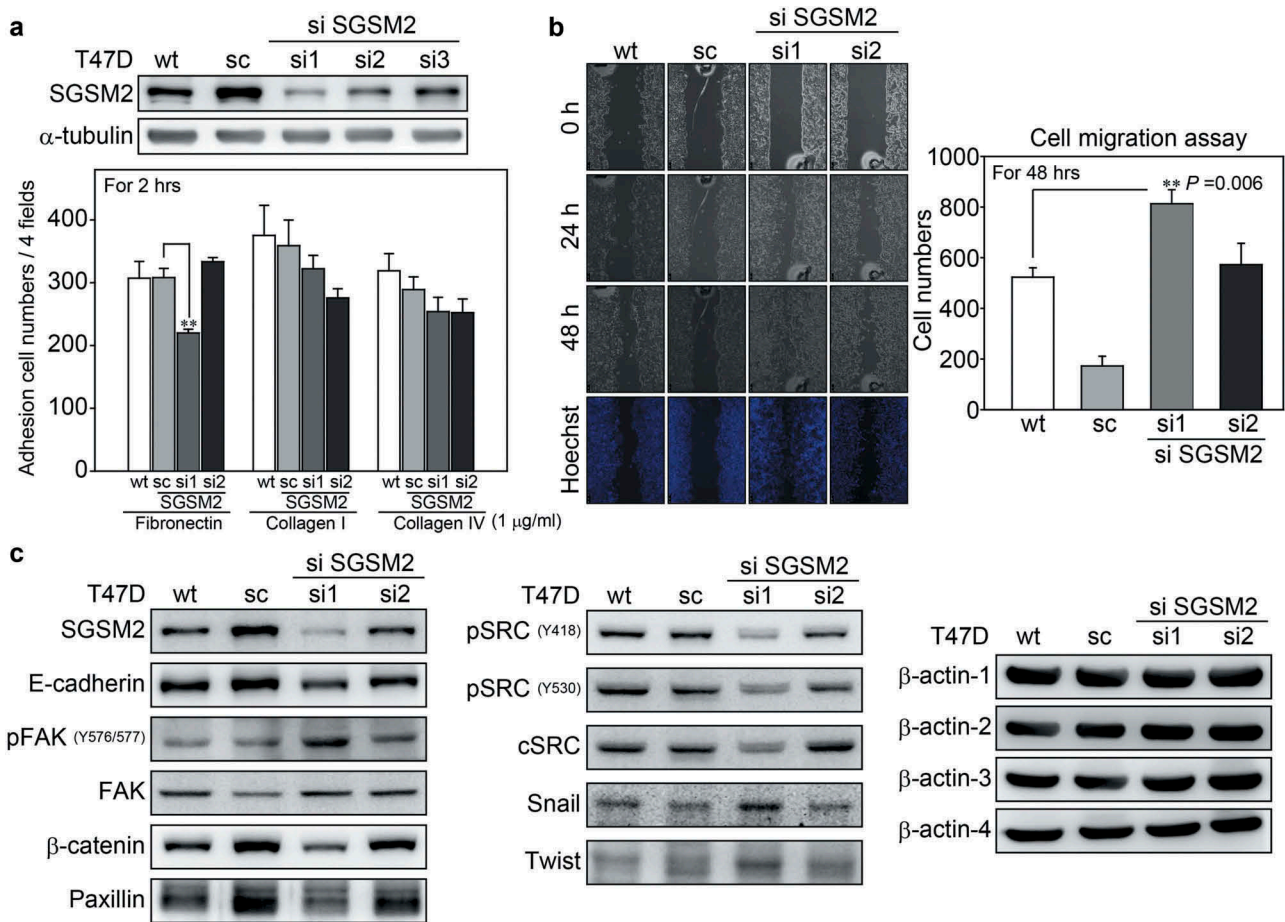


Figure 5. SGSM2 silencing affected T47D cell adhesion and cell migration. (a) The efficiency of SGSM2 knockdown was determined by western blotting (upper panel); sc (scramble), si1, si2, and si3 SGSM2 stable cell lines were collected by G418 selection. The lower panel shows the adhesion abilities of different stable cell lines plated on three types (fibronectin, type I collagen, and type IV collagen; 1 μ g/ml) of ECM proteins. Wt indicates wild-type T47D cells. (b) Cell migration abilities of four types (wt, sc, si1, si2) of T47D cells were examined with wound-healing assays; left panels show the cell migration states at 0, 24, and 48 hours. Hoechst was used to stain the nuclei. The average number of migrated cells is presented in the right panel. (c) The protein levels of E-cadherin, β -catenin, Paxillin, FAK, SRC, Snail, and Twist were detected by western blotting in wt, sc, si1, and si2 T47D cells. β -Actin-1, 2, 3, 4 served as the internal controls. P-values were determined with Student's *t*-test; ** $P < 0.01$. All experiments were repeated more than 3 times ($n > 3$).

increased. Snail and Twist-1 expression was also increased in si1 SGSM2 T47D cells (Figure 5(c)). These results revealed that SGSM2-silenced BC cells exhibit a more migratory phenotype, decreased cell adhesion and improved migration abilities, but why SRC protein was dramatically decreased in si1 SGSM2 T47D cells remains unknown.

SGSM2 interacted with E-cadherin and β -catenin cell-cell adhesion molecules

During the process of EMT, cells become spindle-shaped and exhibit increased intercellular separation, increased motility, and loss of cell-cell adhesion [27]. An E-cadherin/ β -catenin/ α E-catenin complex, also called CCC, is present in the plasma membrane and is

involved in cell-cell adhesion [28]. Based on our above results, we considered that the function of SGSM2 might correlate with cell-cell junctions. EGTA, a Ca^{2+} -specific chelator, can disrupt cadherin-mediated cell-cell adherens junctions, and subsequent restoration of Ca^{2+} ions may re-establish cadherin-mediated cell-cell contacts [29]. Thus, we used these two molecular approaches to perform the immunoprecipitation (IP) experiments. When we pulled down E-cadherin, SGSM2 was also precipitated, which indicated that E-cadherin and SGSM2 have a strong interaction, and EGTA (4 mM) and calcium (Ca^{2+} ; 1.8 mM) ion addition subsequent to EGTA did not affect this interaction (Figure 6(a)). Because β -catenin can conjugate with E-cadherin, we further performed IP with β -catenin and found that SGSM2 could also be brought down

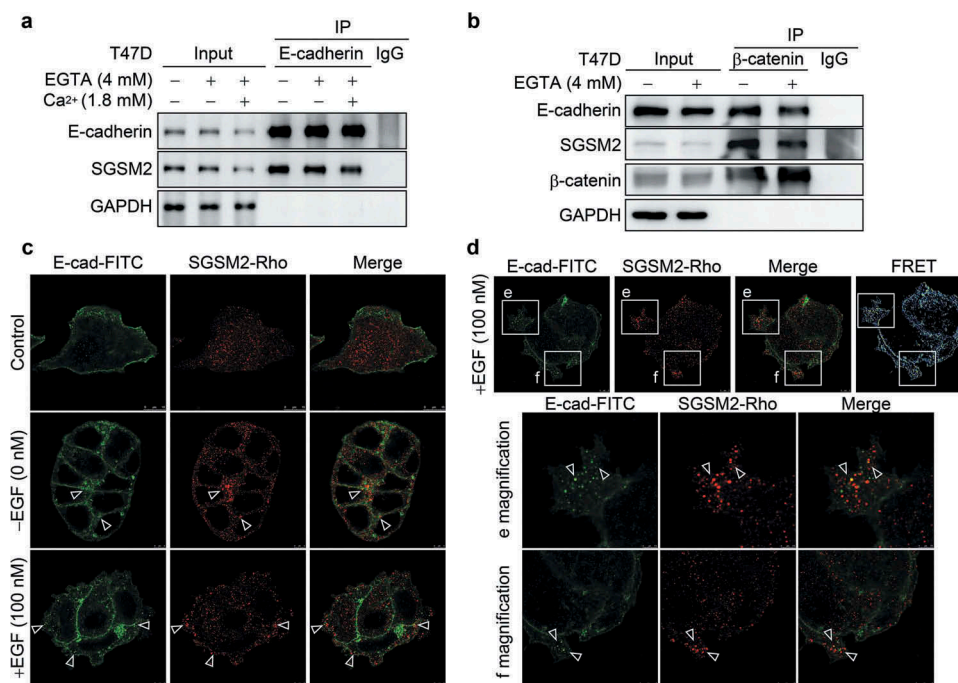


Figure 6. Interaction between SGSM2 and E-cadherin was verified by co-immunoprecipitation and immunofluorescence staining assays. (a) Co-IP of E-cadherin or (b) β -catenin was assessed via western blotting. T47D cells were treated with or without EGTA (4 mM); calcium ions (Ca^{2+}) (1.8 mM) were further added to reform adherent junctions after treatment with EGTA for 30 minutes. Protein complexes were pulled down by anti-E-cadherin or anti- β -catenin antibody and subsequently analysed by western blotting. Irrelevant IgG was used as a negative control. (c) The colocalization of E-cadherin-FITC (green) and SGSM2-rhodamine (red) was detected by IF staining. EGF (100 nM) was used to induce E-cadherin endocytosis. Scale bar of control: 10 μm ; scale bars of EGF – and EGF+: 5 μm . White arrows indicate colocalization of E-cadherin and SGSM2. (d) The colocalization of E-cadherin-FITC and SGSM2-rhodamine was determined by EGF (100 nM) treatment. FRET activity strongly indicated an interaction between SGSM2 and E-cadherin (upper panels; scale bar: 5 μm). Enlarged images of the boxed areas in e and f are shown in the bottom panels. Scale bar of e magnification: 2.5 μm ; scale bars of magnifications: 5 μm .

with β -catenin, even in the presence of EGTA (4 mM) treatment (Figure 6(b)). However, EGTA still had a small effect on the interaction of E-cadherin, β -catenin, and SGSM2 proteins. EGF has been reported to induce focal adhesion disassembly and enhance tumour cell motility through EGFR-activated E-cadherin endocytosis [30,31], and SGSM2 has been reported to interact with RAB family proteins, who function in recycling of vacuoles between the early endosome and plasma membrane [16]. Therefore, we investigated whether SGSM2 is involved in E-cadherin protein endocytosis. In the control T47D cells shown in Figure 6(c) (upper panels), SGSM2 (red) and E-cadherin (green) proteins on the cell adhesion surface strongly interacted, and at cell-cell adhesion junction fields, very strong colocalization between SGSM2 and E-cadherin was found (Figure 6(c), middle panels; arrowheads). This phenomenon was still observed during 100 nM EGF-induced endocytosis of E-cadherin, as shown in Figure 6(c) (bottom panels; arrowheads) and Figure 6(d) (E and F magnifications; arrowheads). These results were convincing because of the strong

Fluorescence resonance energy transfer (FRET) activity observed (Figure 6(d)). To clarify whether SGSM2 is located in endocytic vesicles after EGF treatment, we also performed IF staining using early endosome antigen 1 (EEA1), which is an early endosome marker and SGSM2 antibody. The results indicated positive colocalization of SGSM2 with EEA1 with or without EGF treatment, as shown in Figure S4.

SGSM2 colocalized with phospho-FAK (Y397) at oestrogen-stimulated focal adhesions and ruffling surfaces

To study nascent adhesion formation, cell dissociation buffer was used to harvest MCF-7 cells, which were then placed onto fibronectin-coated glass slides in the absence of serum to synchronize adhesion site formation. After cell seeding for 2 hours, SGSM2 was found to colocalize with phospho-FAK (Y397) at initial adhesion sites (Figure 7(a); upper panels, arrowheads). Particularly at the 6-hour mark of cell seeding, this colocalization

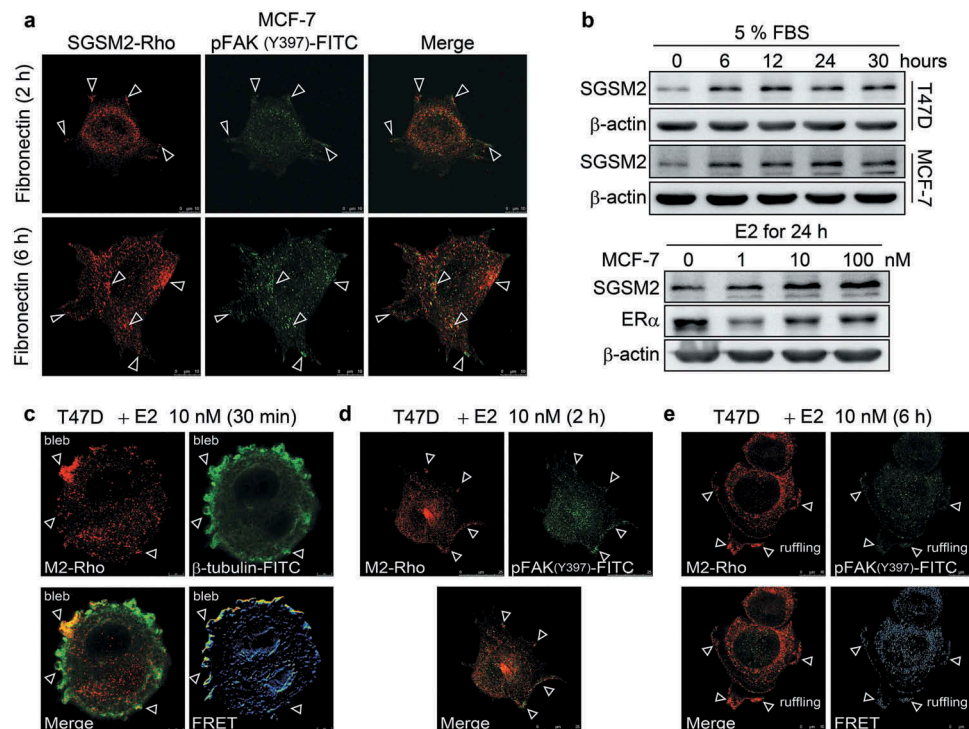


Figure 7. SGSM2 was located with p-FAK (Y397) at the leading edge of oestrogen-induced migrating cells. (a) SGSM2 and p-FAK (Y397) colocalized at focal adhesions in fibronectin-stimulated MCF-7 cells. The upper images were acquired at the 2-hour mark after cell seeding on fibronectin-coated slides; the bottom image was captured at the 6-hour mark after cell seeding. SGSM2 is shown in red (rhodamine), and p-FAK (Y397) is shown in green (FITC). White arrows indicate colocalization of SGSM2 and p-FAK (Y397) at focal adhesion sites. Scale bar, 10 μ m. (b) SGSM2 protein expression was induced in T47D and MCF-7 cells at different times (0, 6, 12, 24, and 30 hours) by 5% FBS (serum) exposure (upper panel). SGSM2 was dose-dependently (0, 1, 10, 100 nM) increased in MCF-7 cells by treatment with oestradiol (E2) (bottom panel). β -Actin was the internal control. (c) Cell bleb formation occurred at the 30-minute mark after E2 (10 nM) exposure. SGSM2 is shown in red (rhodamine), and β -tubulin is shown in green (FITC). A strong interaction was indicated by FRET activity. White arrows indicate colocalization of SGSM2 and β -tubulin. Scale bar, 5 μ m. (d) Focal adhesion formation occurred at the 2-hour mark after E2 (10 nM) exposure; white arrows indicate colocalization of SGSM2 and p-FAK (Y397) at focal adhesion sites. Scale bar, 25 μ m. (e) Cell ruffling formation occurred at the 6-hour mark after E2 (10 nM) exposure; white arrows indicate colocalization of SGSM2 and p-FAK (Y397) at ruffling sites. Scale bar, 10 μ m. (d) (e) SGSM2 is shown in red (rhodamine), and p-FAK (Y397) is shown in green (FITC).

became more visible (Figure 7(a); bottom panels, arrowheads). A 3D image showed that FAK obviously colocalized with SGSM2 on fibronectin-coated glass slides (Figure S5(a)). Because oestrogen was reported to promote endothelial cell and BC cell motility through ER α -activated FAK phosphorylation and the subsequent formation of focal adhesion complexes [32,33], we suggested that SGSM2 protein was expressed relative to ER expression in BC cells (Figure 1(d)). Here, 5% foetal bovine serum (FBS)-induced SGSM2 protein production was determined at the sixth hour after treatment in both T47D and MCF-7 cells (Figure 7(b), upper panels), and we observed that SGSM2 protein levels were dose-dependently (0, 1, 10, 100 nM) increased in MCF-7 cells by 17 β -oestradiol (E2) treatment (Figure 7(b), bottom panels). We next studied SGSM2 protein localization during oestrogen-induced focal adhesion formation. Changes in cellular motility resulted in membrane

blebbing, which was observed at the beginning of treatment with E2 (10 nM) for 30 minutes. FRET activity revealed that SGSM2 (red) strongly colocalized with β -tubulin (green) in the plasma membrane blebs of T47D cells (Figure 7(c), arrowheads), and disruption of the membrane-actin cortex was observed (Figure S5(b)). At the second hour of treatment with E2 (10 nM), phospho-FAK³⁹⁷ (green) and SGSM2 (red) were distributed at the leading edge (Figure 7(d), arrowheads). Moreover, FRET activity also showed that phospho-FAK³⁹⁷ (green) and SGSM2 (red) were colocalized at the E2-induced ruffles formed at the plasma membrane during the sixth hour (Figure 7(e), arrowheads). This evidence indicates that both fibronectin (1 μ g/ml) and E2 (10 nM) treatment could induce SGSM2 and phospho-FAK³⁹⁷ colocalization during the dynamic remodelling of the cytoskeleton and cell membrane and that SGSM2 may be involved in cell motility regulation.

Higher *SGSM2* mRNA levels were found in ER-positive metastatic patients than in those with an ER-negative status

Our study verified that inhibition of *SGSM2* could reduce cell adhesion and increase cancer cell migration; however, we also found that *SGSM2* was involved in modulating E2-induced cell motility. These two results appear contradictory; thus, we analysed the possible effect of *SGSM2* gene expression in BC patients in the TCGA Breast Cancer (BRCA) cohort. Higher *SGSM2* expression was found in metastatic tumour tissues than in primary site tumours (Figure S6(a,b)). We further analysed pathologic Meta status compared with ER status in primary site tumours and observed that *SGSM2* expression correlated only with ER-positive BC patients but not with ER-negative patients (Figure S6(c,d); M1: ER+ vs. ER-, **P = 0.009 and D; M1: ER+ vs. ER-, *P = 0.015). These data definitively confirmed that *SGSM2* is involved in oestrogen-induced cancer cell migration and is regulated by the ER pathway.

Discussion

In 1999, scientists created the ‘full-length long Japan’ (FLJ) collection of sequenced human cDNAs and first reported the complete sequencing and characterization of 21,243 human cDNA clones in 2004 [34]. Hence, three novel proteins (*SGSM1/2/3*) were first identified for their function in modulating the small G protein (RAP and RAB)-mediated signalling pathway in 2007 [16]. In this study, we first determined the *SGSM1/2/3* mRNA expression in BC and normal breast cell lines; however, only *SGSM2* and *SGSM3* were found to be expressed in these cells, and no *SGSM1* expression was observed. This finding was consistent with a previous report that indicated that *SGSM1* is expressed mainly in the brain, heart, and testis [16]. We further investigated *SGSM2* and *SGSM3* mRNA levels in tumours and paired normal tissues from 53 BC patients via RT-PCR. Compared with *SGSM3* expression, *SGSM2* expression in tumours was significantly higher, and its percentage of occurrence in the T > N group was 74%. Based on quantitative real-time PCR, *SGSM2* gene expression in paired tumour tissues was 2-fold higher than that in paired normal tissues from 200 BC patients, and this expression significantly correlated with luminal A type BC rather than the HER2-positive or TNBC types. These data provided evidence that was confirmed not only with our clinical statistics but also using the TCGA Breast Cancer (BRCA) cohort. Moreover, *SGSM2* protein was highly expressed in ER-positive BC cells (BT474, MCF-7, T-47D, and ZR-75) and in ER-positive breast tumour tissues.

Currently, there are still few studies on *SGSM2*. One report indicated that *SGSM2*, also known as RUTBC1, is a Rab9A effector that can promote the GTP hydrolysis of Rab32 and Rab33B proteins [22] and demonstrated that it regulates Rab9A-mediated melanogenic enzyme trafficking in melanocytes through a GAP for Rab32/38 [18,22,35,36]. These findings indicate that *SGSM2* may be involved in transport from late endosomes to the trans-Golgi network; however, it has not been clarified whether *SGSM2* is located on the endomembrane system. Incidentally, we noticed that during the cell culture process, 21 μ M trypsin-EDTA could cleave *SGSM2* protein, and we confirmed that *SGSM2* protein was cleaved by treatment with trypsin-EDTA at concentrations of 21 nM or higher. This phenomenon was found not only in all *SGSM2*-expressing BC cells but also in E-cadherin-expressing cells. We further observed that an approximately 55-kDa fragment of *SGSM2* formed after 1X trypsin-EDTA treatment and verified that *SGSM2* is a plasma membrane protein via a cytosol and membrane extraction assay. According to previous reports and our findings, we proposed that if *SGSM2* is a membrane protein, it might also be located in the endomembrane system and involved in membrane trafficking pathways in the cell. Although trypsinization can induce proteome alterations due to the up- or downregulation of protein expression [37], our results showed that high doses of trypsin (210 and 2100 nM) did not affect *SGSM2* mRNA levels (Figure S2(b)). However, *SGSM2* protein disappeared from the membrane extracts after exposure to high-dose ($\geq 21 \mu$ M) trypsin but not low-dose (<21 nM) trypsin. These data verified that trypsin directly digests *SGSM2* on the cell surface, but *SGSM2* is not affected by trypsin-induced changes in protein expression.

Consistently, the cell adhesion ability of trypsinized T47D cells was significantly decreased compared with non-trypsinized cells on plates coated with different fibronectin concentrations (0.1, 1, and 10 μ g/ml), but these results did not occur on type I- and type-II collagen. In addition, trypsinization also inhibited nicotine- and NNK-induced cell adhesion ability on fibronectin. These results revealed that trypsinization reduced cell adhesion by abolishing anchor molecules on fibronectin but not type I- and type-II collagen substrates. Natural compounds, such as garcinol, curcumin, and nobiletin, have been reported to exhibit anti-metastatic activity through the regulation of EMT-related protein expression [38–42]. We next found that curcuminoids, such as calebin A and 3' PS, which inhibit *SGSM2* protein expression, suppressed the

NNK-induced increase in cell adhesion on a 1 $\mu\text{g}/\text{ml}$ fibronectin-coated dish. We also found that SGSM2 protein was slightly increased by 0.1 μM calebin A treatment but was decreased after 1 and 10 μM calebin A treatment. These results are consistent with the cell adhesion data in which 0.1 μM calebin A combined with NNK increased T47D cell adhesion ability; however, high-dose (1 and 10 μM) calebin A significantly inhibited cell adhesion ability regardless of whether it was combined with NNK. Although there are few studies indicating an inhibitory effect of calebin A on cancer metastasis, we here verified its ability to suppress cancer cell adhesion, and this activity might be associated with SGSM2 protein expression. Furthermore, we observed the T47D si1 cell line, with greater SGSM2 silencing, exhibited a greater capacity to inhibit adhesion (** $P < 0.01$) than the T47D si2 clone cell line, which exhibited slight SGSM2 inhibition. Additionally, SGSM2 knockdown promoted T47D cell migration, which was associated with the upregulation of p-FAK (Y576/577) and epithelial-associated markers (Snail and Twist) and the downregulation of E-cadherin, β -catenin, and Paxillin. By contrast, E-cadherin, β -catenin, and Paxillin were slightly increased in scramble cell lines in which SGSM2 was upregulated, and the cell migration ability was significantly inhibited.

SGSM2 functions as a modulator of RAP proteins, and we know that the RAP family is involved in various cellular phenomena, such as integrin-mediated cell adhesion, cadherin-mediated cell junction formation, and actin dynamics [16]. Our data revealed that SGSM2 knockdown might trigger cell migration by altering the expression of cell-cell junction proteins and inhibiting cell adhesion. Therefore, we hypothesized that SGSM2 is associated with E-cadherin endocytosis. EGTA disrupts E-cadherin-mediated intercellular junctions and induces E-cadherin endocytosis, and this phenomenon is restored by treatment with Ca^{2+} [29]. In our co-IP experiments, E-cadherin and SGSM2 strongly interacted with each other regardless of pretreatment EGTA-induced cell endocytosis formation or the reformation of adherens junctions by further incubation with Ca^{2+} . The same result was observed when a β -catenin antibody was used in a pull-down assay. This evidence demonstrated that SGSM2 directly interacts with E-cadherin/ β -catenin.

EGF induces cell migration and invasion via caveolin-dependent E-cadherin endocytosis and downregulation of caveolin-1 and E-cadherin expression [31]. Under normal conditions, SGSM2 colocalized with E-cadherin at cell junctions. After EGF treatment for 30 minutes, SGSM2 also colocalized with E-cadherin

during EGF-induced endocytosis. Strong energy transfer was observed in the FRET activity assay, demonstrating that SGSM2 might interact with E-cadherin at the cell surface junction and be involved in E-cadherin endocytosis. The ECM protein fibronectin has been shown to enhance the metastatic potential of BC cells [43], and it can stimulate FAK phosphorylation through integrin-mediated signalling pathways during tumour cell migration and invasion [44]. After seeding MCF-7 cells on fibronectin-coated slides and allowing them to adhere for two hours, slight SGSM2 localization with p-FAK (Y397) was observed at the fibronectin-induced focal adhesion position, and this phenomenon became more apparent at the sixth hour. The conspicuous colocalization between FAK and SGSM2 was also observed in the 3D image.

Next, we confirmed that 5% FBS and E2 exposure can stably induce SGSM2 protein expression. Oestrogen has been reported to promote BC cell motility and invasion via FAK phosphorylation, and FAK recruits the small GTPase cdc42, which induces N-WASP phosphorylation [33]. Ligand-induced ER α interacts with the G protein G α_{13} , leading to activation of the small GTPase RhoA and the downstream effector Rho-associated kinase, resulting in myosin phosphorylation and driving actin remodelling [45]. Bleb formation is driven by cell contractions, increases the intracellular pressure and has been determined to occur at the leading edge of moving cells. Three components of the cytoskeleton (microfilaments, microtubules, and intermediate filaments) are required for regulating blebbing, and myosin II contraction in the actin cortex, which is regulated by the small GTPase RhoA, leads to membrane detachment and bleb inflation [46,47]. In the dynamic changes in motility induced by E2, abundant SGSM2 was observed to accumulate with β -tubulin at the plasma membrane blebs at the 30-minute mark; moreover, colocalization of SGSM2 and p-FAK (Y397) was found not only in focal adhesions but also at the leading edge of ruffling and lamellipodia. Herein, we demonstrated that SGSM2 is involved in EGF-induced E-cadherin endocytosis and is associated with E2-induced cancer cell migration, and SGSM2 might be involved in regulation of cytoskeleton dynamics. Interestingly, the BioGRID database, which can be used to predict the physical interaction between SGSM2 and other proteins, was verified by our results. Four of the sixteen physical interactions identified, namely, interactions with CELSR3, EGFR, FNBP1L, and MMP1, were associated with cell migration and invasion (Figure S7(a)), and it is also noteworthy that FNBP1L was found to interact with WASL, CDC42, and CDH1, which are involved in cytoskeleton remodelling and cell-cell junctions (Figure S7(b-d)). This prediction

is consistent with our presumption, but additional data are still needed to further support these findings in future work.

Finally, website databases were used to confirm our findings. Because *SGSM2* and E-cadherin proteins were shown to be highly associated in ER-positive BC cells, we considered that they present similar clinical pathological features in BC. Unexpectedly, *SGSM2* mRNA levels showed a higher distribution in invasive lobular carcinoma (ILC) than in infiltrating ductal carcinoma (IDC) (Figure S8(a), $***P < 0.001$). These data were not consistent with *CDH1* expression data, which was more highly expressed in IDC than in ILC (Figure S8(b), $***P < 0.001$), and even in *CDH1*-positive BC patients, a significant correlation with *SGSM2* was not found (Figure S9(a,b)). However, we observed that one common characteristic of *SGSM2* and *CDH1* is that both are highly expressed in fibroadenoma (Figure S9(c), $*P = 0.002$ and D, $*P = 0.038$). Although fibroadenoma might have the potential to develop into invasive *in situ* carcinoma in women with the *BRCA1* gene mutation [48], the overall risk of fibroadenoma progression to breast carcinoma is very low. In addition, fibroadenoma is a benign breast tumour with proliferation of both epithelial and stromal components, and TCGA data showed higher *SGSM2* gene expression in normal breast tissues than in breast tumour tissues (Figure S6 (a)). Therefore, we examined the relationship between *SGSM2* and *CDH1* expression in normal breast tissues in a TCGA cohort using a Pearson correlation test and partial correlation test. A significant positive correlation between *SGSM2* and *CDH1* is shown in paired normal breast tissues [Sig. (r) = $***(.725)$] but not in paired tumour tissues [Sig. (r) = (.115)] or in all breast tumours [Sig. (r) = $***(-.184)$] (Supplementary Table 2). Moreover, *ERBB2* had the strongest association with *SGSM2* expression in normal breast tissues [Sig. (r) = $***(.877)$], and it appears to be an important factor influencing the relationship between *SGSM2* and *CDH1* (Supplementary Table 2; partial correlation test). More interestingly, the migration-associated markers *SNAI1*, *TWIST1*, *PIK3CA*, and *VIMENTIN* displayed a significantly negative relationship with *SGSM2* in normal breast tissues, but this relationship was not found in breast tumour tissues (Supplementary Table 2). Because BC is a heterogeneous disease that is caused by DNA mutations or epigenetic changes, we conjectured that these phenomena could disrupt the connection between *SGSM2* and other genes in breast tumours, especially the *ERBB2* gene.

Consistently, *SGSM2* exhibited significantly lower expression levels in BC patients with *TP53*, *BRCA2*, or *PIK3R1* (*PIK3CA* suppressed domain) mutation

(Figure S10(a), $***P < 0.001$; B, $***P < 0.001$ and C, $*P = 0.037$), and higher levels of *SGSM2* in BC patients were significantly associated with a low risk of recurrence (Figure S11(a), $**P = 0.002$, CI = 59.92, risk groups hazard ratio = 1.82). Moreover, the ability of the combination of *SGSM2* with *ERBB2* or *MKI67* to predict recurrence-free survival was significantly improved (Figure S11(d), $***P = 0.00019$ and E, $***P = 3.52e-05$). High *ERBB2* or *MKI67* levels along with a low *SGSM2* level in BC patients indicated a high risk of recurrence. In previous experiments, we observed that *SGSM2* had two-fold higher expression in tumours than in normal control tissues from Taiwanese BC patients, but the above statistical data strongly indicated that lower *SGSM2* levels in BC patients could increase tumour recurrence. Although there appears to be two opposing results, according to our clinical analysis, *SGSM2* expression represents a good prognostic phenotype, such as ILC and luminal A type BC. Additionally, a functional assay revealed that loss of *SGSM2* could enhance cancer cell migration. Therefore, *SGSM2* might be a mediator to maintain the equilibrium of cell motility and might play a tumour suppressor role during BC formation initiation.

Conclusions

Our study reveals that *SGSM2* not only interacts with E-cadherin but also participates in cell focal adhesions and cell motility. *SGSM2* is a small G protein modulator that mediates the RAP-signalling pathway and RAB-associated intracellular vesicle transportation [16], and many GTPases, including RhoA, Ras, and Rap1, play an important role in managing cell polarization to drive cell shape changes and motility [29,49]. Thus, we hypothesize that *SGSM2* is involved in E-cadherin endocytosis, cell adhesion, and migration, likely through cooperation with small GTPases. Although additional evidence is needed to further clarify this hypothesis, our novel findings indicate that *SGSM2* is a plasma membrane protein that coordinates cell adhesion and migration.

Material and methods

Tissue collection

Two hundred human BC tissues were obtained from anonymous donors at Taipei Medical University Hospital and Cathay General Hospital, Taipei, Taiwan. The study methodologies conformed to the standards set by the Declaration of Helsinki, and the

study methodologies were approved by the TMU-Joint Institutional Review Board (TMU-JIRB, 20170119). Each sample was divided into paired tumour and normal tissues.

Cell culture

Human mammary gland epithelial adenocarcinoma cell lines (luminal subtype A: BT-483 (ATCC-HTB-121), MCF-7 (ATCC HTB-22), T47D (ATCC HTB-133), and ZR75-1 (ATC CRL-1500); luminal subtype B: BT-474 (ATCC HTB-20); HER2 subtype: AU-565 (ATCC CRL-2351), SKBR3 (ATCC HTB-30), HCC1419 (ATC CRL-2326), HCC1945 (ATC CRL-2338), and MDA-MB-453 (ATCC HTB-131); basal subtype: MDA-MB-231 (ATCC HTB-26), MDA-MB-468 (ATCC HTB-132), and Hs-578T (ATCC HTB-126)), a human melanoma cell line (MDA-MB-435s), and non-tumourigenic immortalized breast epithelial cell line [MCF-10A (ATCC CRL-10317)] were purchased from American Tissue Cell Culture collection (ATCC). MCF-10A cells were maintained under conditions that have been well-established by Xiao-guang Sun et al. [50]. The other cell lines were maintained in DMEM or DMEM/F12 (Thermo Fisher Scientific) supplemented with 10% FBS, Thermo Fisher Scientific), penicillin (100 units/mL), streptomycin (100 µM/mL), and 250 µg/mL amphotericin B at 37°C in a humidified 5% CO₂ incubator.

Quantitative real-time PCR and reverse transcription-polymerase chain reaction (RT-PCR)

Total RNA was extracted from human cell lines and frozen breast tissue specimens using an isothiocyanate-phenol-chloroform procedure according to the TRIzol® reagent manufacturer's protocol (Invitrogen). Complementary DNA (cDNA) was synthesized from 2 µg of total RNA with 0.5 µg of oligo(dT) primers using a reverse transcription kit (ReverTra Ace®; Toyobo). PCR amplification was performed in a 25-µl volume using Blend Taq® -Plus- kit (Toyobo) according to the manufacturer's instructions. The conditions for the PCR were as follows: 94°C for 3 minutes; followed by 30–34 cycles of amplification at 94°C for 30 seconds, 60°C for 30 seconds and 72°C for 30 seconds; and, finally, 72°C for 7 minutes. A portion of breast tissue samples from the original group (n = 50 of 200) was randomly selected for the determination of *SGSM2* expression by RT-PCR. Furthermore, quantitative real-time RT-PCR (LightCycler® 2.0) was used to perform absolute quantitation of *SGSM2* expression, and *β-glucuronidase* (*GUS*) was used to normalize the

SGSM2 gene mRNA levels. The appropriate reagents were purchased in a preformulated kit (LightCycler FastStart DNA Master SYBR Green I; Roche Diagnostics GmbH, Roche Molecular Biochemicals). The primers for *SGSM2*, *SGSM3*, and the internal control *GUS* and *β-actin* were as follows: *SGSM2* forward 5'-ACACCCACTTCTACTTCTGTTATC-3' and reverse 5'-GTCCATGTTGTTGTCACGG-3'; *SGSM3* forward 5'-GCAAGAACGACATCATCACAAT-3' and reverse 5'-CGTCACCGAGTCATCCC-3'; *GUS* forward 5'-AGTGTTCCTGCTAGAATAGATG-3' and reverse 5'-AAACAGCCTGTTTACTTGGAG-3'; *β-actin* forward 5'-TGTACGTTGCTATCCAGGCT-3' and reverse 5'-CTCCTTAATGTCACGCACGA-3'.

Immunohistochemical (IHC) analysis

ER-positive and HER2-negative frozen-embedded blocks of BC tissues were sectioned at thicknesses of 5–7 µm. IHC staining was performed as described in our previous study [51]. The primary anti-*SGSM2* antibody (1:800 dilution; NBP1-93637, Novus Biologicals) and anti-*SGSM3* antibody (1:200 dilution; ab99422, Abcam) were incubated with the slides for 1 hour. Then, the signals were detected and amplified using a DAKO REAL EnVision Detection System and Peroxidase/DAB+ (LSAB2 System-HRP (K0673); Dako Corp.). Finally, histologic human BC tissue specimens were stained with haematoxylin and eosin (H&E).

Western blot assay

For protein extraction, cells were dissociated with enzyme-free cell dissociation solution (S-014-C, Merck KGaA) instead of adherent cells with trypsin-EDTA, and they were subsequently removed with a cell scraper. The cell pellets were further lysed on ice in cell lysis buffer (20 mM Tris-HCl, pH 8.0, 137 mM NaCl, 5 mM EDTA, 5 mM EGTA, 10 mM NaF, 1% Triton X-100, and 10% glycerol) supplemented with protease inhibitors (Roche, Indianapolis, IN, USA) and phosphatase inhibitors (Sigma). The proteins were separated in 10% sodium dodecyl sulphate-polyacrylamide gel electrophoresis (SDS-PAGE) gels and transferred to polyvinylidene difluoride membranes (PVDF). The following primary mouse monoclonal antibodies were incubated with the membranes at a 1:4000 dilution for 2 hours: anti-glyceraldehyde 3-phosphate dehydrogenase (GAPDH) (sc-32233, Santa Cruz Biotechnology); and anti-*β-actin* and anti-*α-tubulin* (Santa Cruz Biotechnology). The following primary antibodies were used at a 1:1000 dilution for 2 hours: rabbit polyclonal anti-*SGSM2* (NBP1-93637,

Novus Biologicals); anti- β -catenin (GTX101435, GeneTex), anti-SRC, anti-SNAI1 (C15D3) (#3879, Cell Signalling Technology); goat anti-SGSM3 (ab99422, Abcam); mouse monoclonal anti-Twist (ab175430, Abcam); anti-E-cadherin (610182, BD Biosciences); and anti-FAK (sc-1688, Santa Cruz Biotechnology). The membranes were then incubated with secondary HRP-conjugated anti-mouse or anti-rabbit IgG (Santa Cruz Biotechnology) at a 1:4000 dilution for 1 hour. GAPDH, β -actin, and α -tubulin expression levels were used as protein loading controls.

Cytosol and membrane protein extraction

Cells were lysed in homogenization buffer (20 mM Tris (pH 7.5), 5 mM EGTA, and 20 mM EDTA) containing protease inhibitors and then disrupted by gentle repeated pipetting through a syringe 30 times on ice. After centrifugation at 12000 rpm for 10 minutes at 4°C, the supernatant, which was the cytoplasmic fraction, was transferred to a new microfuge tube, and the cell pellets were extracted for membrane proteins. After the pellet was washed 2 times, it was lysed in cell lysis buffer as described in the western blotting protocol section and further disrupted every 5 minutes for 45 minutes using a vortex mixer. After centrifugation at 12000 rpm for 30 minutes at 4°C, the supernatant was harvested as the membrane fraction. Finally, cytoplasmic and membrane fractions were examined via 10% SDS-PAGE gels.

Cell-matrix adhesion assays

To prepare coated plates, different concentrations (0, 0.1, 1, or 10 μ g/ml) of extracellular matrix (ECM) proteins (fibronectin, collagen I, and collagen IV purchased from Sigma-Aldrich) were evenly incubated in 12-well plates at 37°C for 3 hours. After incubation, the solutions were removed from each well, and the wells were blocked with 0.2% BSA at 37°C for another 1 hour; the plates were washed with PBS 2 times and further dried in an incubator overnight. For the adhesion assay, cells were detached with enzyme-free cell dissociation solution or 21 μ M trypsin-EDTA (1X) (Thermo Fisher Scientific), and then 6×10^4 T47D cells were seeded in a 12-well plate for a 2-hour incubation. Unbound cells were removed by gently washing with PBS 2 times, and adherent cells were fixed with 4% formaldehyde and stained with Hoechst 33342 dye. Cells were washed with PBS and imaged using a 4X objective on a Leica DMI 4000B fluorescence

microscope (Leica Microsystems). For different experimental observations, cells were treated with different concentrations of nicotine (0, 1, 10, or 100 μ M), NNK (0, 10, 100, or 1000 nM), or 10 μ M natural compounds (curcumin, calebin A, or 3' PS).

Establishment of stable SGSM2 siRNA-expressing cell lines

Scramble (sc) and RNAi (si) sequences for SGSM2 were designed using OligoEngine 2.0 software. At least two independent RNAi sequences were used to ablate SGSM2 expression in T47D cells. All sequences were cloned into a pSUPER.retro.neo+gfp vector followed by pSUPER RNAi System Protocols (OligoEngine Co.). T47D cells were transfected with the SGSM2 pSUPER-si1, si2, and pSUPER-sc vectors by electroporation with a Neon® system (Thermo Fisher Scientific Inc.). To select stable cell lines, cells were treated with 2.5 mg/mL G418, and clones were isolated after 25–30 days in selection medium to ensure G418-resistant clone formation. The plasmids were constructed using the following sequences: SGSM2 si1 target sequence, 5'-TCCGATGAAAGACGCTGGT-3' and SGSM2 si2 target sequence, 5'-CCTGCACCGCATAGACAAG-3'; SGSM2 scramble target sequence, 5'-GTATGGA GGCACATACTCG-3'.

Wound-healing migration assay

A culture insert (Ibidi GmbH) was used to generate a 500 ± 50 - μ m gap and placed in each well of 12-well plates; then, 3.5×10^4 T47D cells stably expressing SGSM2 si1, si2 or scramble vectors were seeded into both sides of each insert. After cell seeding for 24 hours, we removed all the culture inserts, exchanged the medium for new growth medium, and imaged cell migration at 0, 24, and 48 hours. Cells were fixed with 4% formaldehyde and stained with Hoechst 33342 dye. Images of all movement in the wound area were captured with a 10X objective on a Leica DMI 4000B fluorescence microscope.

Co-immunoprecipitation (Co-IP)

Cells were lysed on ice in RIPA lysis buffer (20 mM Tris-HCl (pH 7.5), 150 mM NaCl, 1 mM Na₂EDTA, 1 mM EGTA, 1% NP-40, 1% sodium deoxycholate, 2.5 mM sodium pyrophosphate, 1 mM β -glycerophosphate, 1 mM Na₃VO₄, 1 μ g/ml leupeptin, 0.5 M sodium orthovanadate, and 200 μ M PMSF). Cell lysates were further disrupted 3 times over 150 minutes using a vortex mixer

and then spun down at 12000 rpm for 30 minutes. Protein lysates containing equal amounts of total protein (~2 mg) were incubated with 2 µg of specific antibodies against E-cadherin and β-catenin overnight at 4°C, and the mixture was further incubated with protein A/G agarose beads (EMD Millipore) for 2 hours at 4°C. Thereafter, the samples were washed four times with PBS and examined with 10% SDS-PAGE gels. In parallel, an equal amount of nonspecific IgG was used as the negative control. In addition, 4 mM EGTA was used to disrupt E-cadherin-mediated cell-cell contacts, and 1.8 mM Ca²⁺ was used to reform adherent junctions; both experiments were performed using a well-established procedure [29].

Immunofluorescence (IF) staining

Cells were seeded on glass slides for 24 hours and then fixed with 4% paraformaldehyde (Merck) for 5 minutes at room temperature. The fixed cells were rinsed with PBS 3 times and incubated in blocking solution (10% FBS in PBS) for 30 minutes. Cells were then incubated with primary antibodies (anti-SGSM2, anti-E-cadherin, anti-EEA1, anti-p-FAK(Y397), and anti-β-tubulin at 1:200 dilution and Phalloidin-iFluor 488) for 2 hours and further incubated with the specific secondary antibody for 1 hour. Finally, the samples were mounted with Gel Mount (Sigma-Aldrich) and imaged using confocal microscopy (Leica TCS SP5, Leica). Mouse anti-β-tubulin antibody was purchased from GeneTex company (GTX11307). The secondary antibodies were purchased from Jackson ImmunoResearch Lab Co. Phalloidin-iFluor 488 (ab176753, Abcam) or rhodamine phalloidin (# PHDR1, Cytoskeleton Inc.) were used for staining F-actin, which was performed according to the manufacturer's instructions.

Fluorescence resonance energy transfer (FRET)

The acceptor bleaching FRET method was used according to the manufacturer's instructions (FRET Wizards in the Leica Application suite). Briefly, the initial donor (FITC 488 nm) image represents donor fluorescence in the presence of the acceptor rhodamine. After complete photo-bleaching of the acceptor, a second donor image was collected.

Statistical analysis

The cell numbers in the cell adhesion and cell migration assays were determined using ImageJ software. All data are presented as the mean±S.E.M. of more than three independently repeated experiments. SGSM2

mRNA expression in paired normal vs. tumour tissues from BC patients was compared with paired t-tests. Independent t-tests (Welch's t-test for heterogeneous variance) were used to compare the differences between two groups, and one-way ANOVA (LSD, Scheffe, and Tukey HSD test for homogeneity of variance; Dunnett T3 and Games-Howell test for heterogeneous variance) was used to compare differences among three or more groups. A Pearson correlation test was used to analyse the correlation of SGSM2 and CDH1 with the expression of various genes; a partial correlation test was used to verify the association among ERBB2, SGSM2, and CDH1 expression in normal tissue samples. All statistical comparisons were performed using Sigma Plot graphing software and Statistical Package for the Social Sciences v.11.0.0 (SPSS). A P-value of 0.05 or less indicated statistical significance.

Abbreviations

| | |
|--------|--|
| SGSM | small G protein signalling modulator |
| PCR | polymerase chain reaction |
| RT-PCR | reverse transcription PCR |
| EGTA | ethylene glycol tetraacetic acid |
| BC | breast cancer |
| EMT | epithelial-mesenchymal transition |
| ER | oestrogen receptor |
| FGF | fibroblast growth factor |
| TGF-β | transforming growth factor β |
| EGF | epidermal growth factor |
| IGF1 | insulin-like growth factor-1 |
| TNFα | tumour necrosis factor-α |
| MMPs | metalloproteinases |
| HGF | hepatocyte growth factor |
| SF | scatter factor |
| Rap | Ras-associated protein |
| RAPID | RAP-interacting domain |
| GAP | GTPase-activating protein |
| FNBP1L | formin-binding protein 1-like |
| WASL | Wiskott-Aldrich syndrome-like |
| CDC42 | cell division cycle 42 |
| CDH1 | cadherin 1 |
| GUS | β-glucuronidase |
| HER2 | human epidermal growth factor receptor 2 |
| IHC | immunohistochemistry |
| GAPDH | glyceraldehyde 3-phosphate dehydrogenase |
| ECM | extracellular matrix |
| FRET | fluorescence resonance energy transfer |
| FITC | fluorescein isothiocyanate |
| PR | progesterone receptor |
| IP | immunoprecipitation |
| FBS | foetal bovine serum |
| E2 | 17β-estradiol |
| LN | lobular neoplasia |
| ILC | invasive lobular carcinoma |
| IDC | invasive ductal carcinoma |
| FAK | focal adhesion kinase |

Disclosure statement

No potential conflict of interest was reported by the authors.

Funding

This work was supported by the Health and Welfare Surcharge of Tobacco Products grant [MOHW107-TDU-B-212-114014]; the TMU Research Center of Cancer Translational Medicine from The Featured Areas Research Center Program within the framework of the Higher Education Sprout Project by the Ministry of Education (MOE) in Taiwan [none]; the Ministry of Science and Technology, Taiwan [MOST105-2320-B038-053-MY3] and [MOST106-2320-B-038-046] awarded to Dr. Ho, [MOST106-2314-B-038-053-MY3] awarded to Dr. Tu, [MOST106-2320-B038-061-MY3] awarded to Dr. Chen, and [MOST104-2314-B-038-059-MY3] awarded to Dr. Wu; and Taipei Medical University [TMU104-AE1-B12] awarded to Dr. Chen.

References

- [1] Heerboth S, Housman G, Leary M, et al. EMT and tumor metastasis. *Clin Transl Med.* 2015;4:6.
- [2] Mitra SK, Hanson DA, Schlaepfer DD. Focal adhesion kinase: in command and control of cell motility. *Nat Rev Mol Cell Biol.* 2005;6:56–68.
- [3] Canel M, Serrels A, Frame MC, et al. E-cadherin-integrin crosstalk in cancer invasion and metastasis. *J Cell Sci.* 2013;126:393–401.
- [4] Kumar S, Das A, Sen S. Extracellular matrix density promotes EMT by weakening cell-cell adhesions. *Mol Biosyst.* 2014;10:838–850.
- [5] Friedl P, Wolf K. Tumour-cell invasion and migration: diversity and escape mechanisms. *Nat Rev Cancer.* 2003;3:362–374.
- [6] Barrallo-Gimeno A, Nieto MA. The Snail genes as inducers of cell movement and survival: implications in development and cancer. *Development.* 2005;132:3151–3161.
- [7] Wang Y, Shi J, Chai K, et al. The role of Snail in EMT and tumorigenesis. *Curr Cancer Drug Targets.* 2013;13:963–972.
- [8] Wu Y, Ginther C, Kim J, et al. Expression of Wnt3 activates Wnt/beta-catenin pathway and promotes EMT-like phenotype in trastuzumab-resistant HER2-overexpressing breast cancer cells. *Mol Cancer Res.* 2012;10:1597–1606.
- [9] Li CW, Xia W, Huo L, et al. Epithelial-mesenchymal transition induced by TNF-alpha requires NF-kappaB-mediated transcriptional upregulation of Twist1. *Cancer Res.* 2012;72:1290–1300.
- [10] Chavrier P, Parton RG, Hauri HP, et al. Localization of low molecular weight GTP binding proteins to exocytic and endocytic compartments. *Cell.* 1990;62:317–329.
- [11] Zheng G, Lyons JG, Tan TK, et al. Disruption of E-cadherin by matrix metalloproteinase directly mediates epithelial-mesenchymal transition downstream of transforming growth factor-beta1 in renal tubular epithelial cells. *Am J Pathol.* 2009;175:580–591.
- [12] Parikh RA, Wang P, Beumer JH, et al. The potential roles of hepatocyte growth factor (HGF)-MET pathway inhibitors in cancer treatment. *Onco Targets Ther.* 2014;7:969–983.
- [13] Gao L, Feng Y, Bowers R, et al. Ras-associated protein-1 regulates extracellular signal-regulated kinase activation and migration in melanoma cells: two processes important to melanoma tumorigenesis and metastasis. *Cancer Res.* 2006;66:7880–7888.
- [14] Kawauchi T. Regulation of cell adhesion and migration in cortical neurons: not only Rho but also Rab family small GTPases. *Small GTPases.* 2011;2:36–40.
- [15] Takai Y, Sasaki T, Matozaki T. Small GTP-binding proteins. *Physiol Rev.* 2001;81:153–208.
- [16] Yang H, Sasaki T, Minoshima S, et al. Identification of three novel proteins (SGSM1, 2, 3) which modulate small G protein (RAP and RAB)-mediated signaling pathway. *Genomics.* 2007;90:249–260.
- [17] Itoh T, Satoh M, Kanno E, et al. Screening for target Rabs of TBC (Tre-2/Bub2/Cdc16) domain-containing proteins based on their Rab-binding activity. *Genes Cells.* 2006;11:1023–1037.
- [18] Marubashi S, Shimada H, Fukuda M, et al. RUTBC1 functions as a GTPase-activating protein for Rab32/38 and regulates melanogenic enzyme trafficking in melanocytes. *J Biol Chem.* 2016;291:1427–1440.
- [19] Pannekoek WJ, Kooistra MR, Zwartkruis FJ, et al. Cell-cell junction formation: the role of Rap1 and Rap1 guanine nucleotide exchange factors. *Biochim Biophys Acta.* 2009;1788:790–796.
- [20] Subramani D, Alahari SK. Integrin-mediated function of Rab GTPases in cancer progression. *Mol Cancer.* 2010;9:312.
- [21] McSherry EA, Brennan K, Hudson L, et al. Breast cancer cell migration is regulated through junctional adhesion molecule-A-mediated activation of Rap1 GTPase. *Breast Cancer Res.* 2011;13:R31.
- [22] Nottingham RM, Ganley IG, Barr FA, et al. RUTBC1 protein, a Rab9A effector that activates GTP hydrolysis by Rab32 and Rab33B proteins. *J Biol Chem.* 2011;286:33213–33222.
- [23] Nottingham RM, Pusapati GV, Ganley IG, et al. RUTBC2 protein, a Rab9A effector and GTPase-activating protein for Rab36. *J Biol Chem.* 2012;287:22740–22748.
- [24] Gankhuyag N, Lee KH, Cho JY. The role of Nitrosamine (NNK) in breast cancer carcinogenesis. *J Mammary Gland Biol Neoplasia.* 2017;22:159–170.
- [25] Dasgupta P, Rizwani W, Pillai S, et al. Nicotine induces cell proliferation, invasion and epithelial-mesenchymal transition in a variety of human cancer cell lines. *Int J Cancer.* 2009;124:36–45.
- [26] Serrano-Gomez SJ, Maziveyi M, Alahari SK. Regulation of epithelial-mesenchymal transition through epigenetic and post-translational modifications. *Mol Cancer.* 2016;15:18.
- [27] Morra L, Moch H. Periostin expression and epithelial-mesenchymal transition in cancer: a review and an update. *Virchows Arch.* 2011;459:465–475.
- [28] van Roy F, Berx G. The cell-cell adhesion molecule E-cadherin. *Cell Mol Life Sci.* 2008;65:3756–3788.
- [29] Balzac F, Avolio M, Degani S, et al. E-cadherin endocytosis regulates the activity of Rap1: a traffic light

- GTPase at the crossroads between cadherin and integrin function. *J Cell Sci.* **2005**;118:4765–4783.
- [30] Kowalczyk AP, Nanes BA. Adherens junction turnover: regulating adhesion through cadherin endocytosis, degradation, and recycling. *Subcell Biochem.* **2012**;60:197–222.
- [31] Lu Z, Ghosh S, Wang Z, et al. Downregulation of caveolin-1 function by EGF leads to the loss of E-cadherin, increased transcriptional activity of beta-catenin, and enhanced tumor cell invasion. *Cancer Cell.* **2003**;4:499–515.
- [32] Sanchez AM, Flamini MI, Zullino S, et al. Estrogen receptor- α promotes endothelial cell motility through focal adhesion kinase. *Mol Hum Reprod.* **2011**;17:219–226.
- [33] Sanchez AM, Flamini MI, Baldacci C, et al. Estrogen receptor- α promotes breast cancer cell motility and invasion via focal adhesion kinase and N-WASP. *Mol Endocrinol.* **2010**;24:2114–2125.
- [34] Saadat N, Gupta SV. Potential role of garcinol as an anticancer agent. *J Oncol.* **2012**;2012:647206.
- [35] Ota T, Suzuki Y, Nishikawa T, et al. Complete sequencing and characterization of 21,243 full-length human cDNAs. *Nat Genet.* **2004**;36:40–45.
- [36] Carroll KS, Hanna J, Simon I, et al. Role of Rab9 GTPase in facilitating receptor recruitment by TIP47. *Science.* **2001**;292:1373–1376.
- [37] Barbero P, Bittova L, Pfeffer SR. Visualization of Rab9-mediated vesicle transport from endosomes to the trans-Golgi in living cells. *J Cell Biol.* **2002**;156:511–518.
- [38] Huang HL, Hsing HW, Lai TC, et al. Trypsin-induced proteome alteration during cell subculture in mammalian cells. *J Biomed Sci.* **2010**;17:36.
- [39] Cheng HL, Hsieh MJ, Yang JS, et al. Nobiletin inhibits human osteosarcoma cells metastasis by blocking ERK and JNK-mediated MMPs expression. *Oncotarget.* **2016**;7:35208–35223.
- [40] Ahmad A, Sarkar SH, Bitar B, et al. Garcinol regulates EMT and Wnt signaling pathways in vitro and in vivo, leading to anticancer activity against breast cancer cells. *Mol Cancer Ther.* **2012**;11:2193–2201.
- [41] Mukherjee S, Mazumdar M, Chakraborty S, et al. Curcumin inhibits breast cancer stem cell migration by amplifying the E-cadherin/beta-catenin negative feedback loop. *Stem Cell Res Ther.* **2014**;5:116.
- [42] Tyagi AK, Prasad S, Majeed M, et al. a novel component of turmeric, suppresses NF-kappaB regulated cell survival and inflammatory gene products leading to inhibition of cell growth and chemosensitization. *Phytomedicine.* **2017**;34:171–181.
- [43] Bartsch JE, Staren ED, Appert HE. Adhesion and migration of extracellular matrix-stimulated breast cancer. *J Surg Res.* **2003**;110:287–294.
- [44] Meng XN, Jin Y, Yu Y, et al. Characterisation of fibronectin-mediated FAK signalling pathways in lung cancer cell migration and invasion. *Br J Cancer.* **2009**;101:327–334.
- [45] Simoncini T, Scorticati C, Mannella P, et al. Estrogen receptor α interacts with Galpha13 to drive actin remodeling and endothelial cell migration via the RhoA/Rho kinase/moesin pathway. *Mol Endocrinol.* **2006**;20:1756–1771.
- [46] Hagmann J, Burger MM, Dagan D. Regulation of plasma membrane blebbing by the cytoskeleton. *J Cell Biochem.* **1999**;73:488–499.
- [47] Charras GT, Hu CK, Coughlin M, et al. Reassembly of contractile actin cortex in cell blebs. *J Cell Biol.* **2006**;175:477–490.
- [48] Yang X, Kandil D, Cosar EF, et al. Fibroepithelial tumors of the breast: pathologic and immunohistochemical features and molecular mechanisms. *Arch Pathol Lab Med.* **2014**;138:25–36.
- [49] Le Clainche C, Carlier MF. Regulation of actin assembly associated with protrusion and adhesion in cell migration. *Physiol Rev.* **2008**;88:489–513.
- [50] Sun XG, Rotenberg SA. Overexpression of protein kinase Calpha in MCF-10A human breast cells engenders dramatic alterations in morphology, proliferation, and motility. *Cell Growth Differ.* **1999**;10:343–352.
- [51] Cheng TC, Tu SH, Chen LC, et al. Down-regulation of alpha-L-fucosidase 1 expression confers inferior survival for triple-negative breast cancer patients by modulating the glycosylation status of the tumor cell surface. *Oncotarget.* **2015**;6:21283–21300.